ISSN 1027-4510, Journal of Surface Investigation: X-ray, Synchrotron and Neutron Techniques, 2021, Vol. 15, No. 3, pp. 570–574. © Pleiades Publishing, Ltd., 2021.
Russian Text © The Author(s), 2021, published in Poverkhnost', 2021, No. 6, pp. 33–38.

Local Atomic and Electronic Structure of Iron-Sulfide Nanosheets

M. A. Soldatov[a], *, P. V. Medvedev[a], I. E. Gorban[a], Q. Liu[b], S. Wei[b], and A. V. Soldatov[a]

[a] *Smart Materials Research Institute, Southern Federal University, Rostov-on-Don, 344090 Russia*

[b] *National Synchrotron Radiation Laboratory, University of Science and Technology of China, Hefei, Anhui, 230029 China*

**e-mail: mikhail.soldatov@gmail.com*

Received September 26, 2020; revised December 22, 2020; accepted December 27, 2020

Abstract—In this paper, we calculate the geometry and band structure of iron sulfide (mackinawite) nanosheets. This material is one of the representatives of a new class of two-dimensional nanocatalysts for the hydrogen evolution reaction. Calculations show the absence of a band gap for model structures of crystalline and nanoscale mackinawite. In the model of oxidized nanoscale mackinawite, half of the sulfur atoms are replaced by oxygen atoms, and the band gap is 0.37 eV. The band-gap broadening can explain the appearance of catalytic activity in oxidized nanoscale mackinawite. The X-ray absorption spectra show a high sensitivity of the method to changes in the local atomic environment, especially in the first coordination sphere of iron atoms. The calculated model spectra allow determination of the features of the local atomic and electronic structure of the nanoscale mackinawite surface during the hydrogen evolution reaction.

Keywords: surface, liquid-solid interface, iron sulfide, materials for energy conversion, water splitting reaction, two-dimensional catalysts, XANES, hydrogen evolution reaction, local atomic structure, electronic structure

DOI: 10.1134/S1027451021030320

INTRODUCTION

Some time ago, global climate change moved from the position of scientists' warnings [1, 2] into the area which nonclimate research industries face [3]. Climatic changes are associated with a systematic increase in the level of greenhouse gases: carbon dioxide, methane, nitrogen oxides, and others. A significant contribution to the emission of greenhouse gases is made by the power industry built on the basis of such combustible energy sources as coal, oil, and gas. It should be noted that greenhouse gases are actively emitted both as a result of the operation of power plants and when fuel is burned in the engines of vehicles. Thus, the development of clean energy is one of the most important tasks to slow down climate change and preserve the environment. An important issue lies both in obtaining energy from renewable sources and efficiently converting and storing it. A long-developed area of renewable energy is the use of solar energy. A comprehensive solution to this issue involves the conversion of solar energy into chemical fuel for further use in fuel cells. Due to its high specific energy-storage efficiency, molecular hydrogen is a promising type of chemical fuel. Cells for the direct conversion of solar energy into chemical energy through the water splitting reaction have been on the market for a long time. However, existing platinum-based catalysts have high costs [4], which can increase even higher with full-scale advancement of the technology. For wide application of the technology, it is necessary to solve important materials science problems: switching from platinum catalysts to catalysts based on common elements while maintaining the stability and efficiency of platinum catalysts.

Nanoobjects based on compounds of inexpensive and widespread transition metals can replace platinum catalysts [4]. Their band gap can vary within the range 1–3 eV [5], which allows absorption of the main part of the visible-light spectrum for the efficient generation of electron-hole pairs. Nanostructured materials have a large surface area and can contain ordered pores. This structure can provide a high rate of charge transfer and the availability of active catalytic sites for electrolyte ions. This is what makes nanomaterials based on transition-metal compounds excellent candidates for energy storage [6]. In the photocatalytic hydrogen evolution reaction, a key stage is the generation of photoelectrons and "holes," as well as their subsequent movement to the catalytically active surface for reduction with the subsequent formation of molecular hydrogen. The separation efficiency of electron-hole pairs may decrease because of the low electrical conductivity and short diffusion length of the material. To increase the efficiency of catalysts, it is advisable to reduce their thickness to a value comparable to the transfer distance of electron-hole pairs in the material.

On account of the low price and abundance of iron, iron sulfide has a high potential for use. Studies show the effectiveness of crystalline iron disulfide for catalysis of the hydrogen evolution reaction [7–11]. However, in terms of efficiency and stability, the studied catalysts are significantly inferior to platinum. Nanoscale catalysts are more promising [12]. For example, a nanoscale catalyst based on porous iron and iron sulfide [13] showed a stability and efficiency superior to platinum analogues. Moreover, catalysts can be obtained from a single material based on porous iron and iron sulfide, exhibiting a high efficiency for both the hydrogen evolution reaction and the oxygen evolution reaction. Another approach that allows a high efficiency to be obtained is the doping of iron-sulfide nanosheets with cobalt [14].

A detailed analysis of the mechanism of action and an increase in the quantum efficiency of catalysts based on nanostructured iron sulfide requires a deep understanding of the fundamental relations between the parameters of its structure and physicochemical properties. Data on the band structure, density of states, effective mass of charge carriers, and periodic structure can be obtained by density-functional-theory calculations. The methods of X-ray diffraction, transmission and scanning electron microscopy, X-ray photoelectron spectroscopy, and X-ray absorption spectroscopy are often used for comprehensive analysis of a structure. The advantages of absorption spectroscopy include elemental selectivity, sensitivity to the local environment of atoms in structures without long-range order, and the ability to obtain data in the operando mode, i.e., under real conditions of the studied catalytic reaction. X-ray absorption spectroscopy data are generally divided into two areas, which are processed using different approaches. Analysis of the EXAFS (Extended X-Ray Absorption Fine Structure) spectra allows the coordination numbers and distances to several coordination spheres to be specified by fitting the parameters. The theoretical analysis of X-Ray absorption spectra XANES (X-Ray Absorption Near-Edge Structure) can, in principle, provide important information about such features of the local atomic and electronic structure of a material as the charge state, interatomic distances, and bond angles. Artificial-intelligence methods for analyzing the XANES spectra allow structure data to be obtained even without measuring reference compounds [15].

In this study, the band structure, density of states, and X-ray absorption spectra were calculated for model structures of crystalline and nanoscale iron sulfide.

CALCULATION METHODS

The geometry and band structures of mackinawite were calculated by density functional theory using the BAND software package [16–20]. Analytical energy gradients for systems with translation invariance are formulated based on the Kohn-Sham density functional theory. Energy gradients are implemented in the BAND program, which directly uses the basis set of Bloch functions consisting of numerically calculated atomic orbitals and Slater-type orbitals [21].

When developing the calculation method, the calculations were performed using exchange-correlation functionals of various types. In particular, the generalized gradient approximation (GGA : BLYP [22, 23]) and the meta-GGA group functionals approximation (SCAN) [24], which showed good agreement with the experimental data for nanoscale cobalt-metahydroxide sheets [25], were considered. A correction for density gradients in the case of the approximation of generalized gradients and the dependence on the kinetic energy and the absence of empirical parameters [24] in the case of functionals of the meta-GGA group were used. The basis sets consisted of atomic orbitals DZP (two-exponential atomic orbitals with the addition of polarization functions) obtained by numerically solving the Kohn-Sham equations for isolated spherical atoms and supplemented by a set of Slater orbitals.

The XANES spectra were calculated by the finite difference method implemented in the fdmnes program [26–28]. This approach made it possible to avoid the muffin-tin approximation and use the "full" potential of the system for calculating the XANES spectra. This approach has proven itself in the case of systems with pronounced covalent bonds or those that contain large interfaces in the study of porous materials based on metal-organic frame structures [29] and cobalt metahydroxide [25].

RESULTS AND DISCUSSION

Mackinawite (FeS) is a finely dispersed, layered, and water-insoluble compound. It forms black crystals of tetragonal syngony, the space group is $P4/nmm$, and the cell parameters are $a = 0.36753$ nm and $c = 0.50328$ nm (COD database, no. 9011800 [30]). The layering of the structure is clear when viewed perpendicular to the c axis (Fig. 1a). The distance between sulfur atoms in two adjacent layers is ~2.41 Å. The first coordination sphere of the iron atom consists of four sulfur atoms (Fig. 1b), forming an almost ideal tetrahedron, the interatomic distances are $R_{Fe-S} = 2.25(6)$ Å. The second coordination sphere is located at $R_{Fe-S} = 2.95(8)$ Å and consists of four iron atoms (Fig. 1c). In the case of considering two-dimensional nanosheets of iron sulfide in water, almost all of the material is the interface between the liquid and the solid. In this case, there are various models describing the active sites of nanostructured 2D catalysts. It should be noted that mackinawite in its pure form does not exhibit pronounced catalytic properties for the hydrogen evolution reaction. The catalytic properties are due to mackinawite oxidation [13]. Therefore, it is expected that the hydrogen evolution reaction will take place at oxygen atoms replacing sulfur atoms.

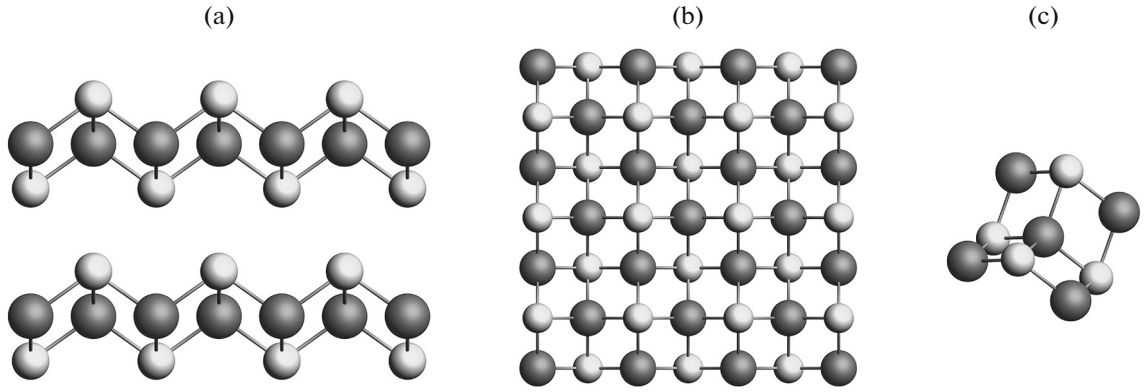

Fig. 1. Image of the periodic structure of mackinawite (a) along and (b) perpendicular to the *c* axis. (c) Image of the local atomic structure of the iron environment. Iron atoms are large dark gray balls, and sulfur atoms are light gray balls.

To calculate the geometry and band structure, we constructed three models of: the structures of crystalline mackinawite, nanoscale mackinawite, and oxidized nanoscale mackinawite. The structure of crystalline mackinawite was taken from an open crystallographic database [30]. To create a model structure of nanoscale mackinawite, a supercell based on the crystal structure was built. For this purpose, a section along the (001) plane was made in such a way that sulfur atoms were on the surface. The supercell consisted of S–Fe–S single layers separated by a distance of 15 Å. Optimization of the geometric structure of the crystalline and nanoscale mackinawite did not show significant changes. Calculations of the forbidden gap based on electron density functional theory make it possible to state the absence of a forbidden gap in crystalline and nanoscale mackinawite. Catalytically active sites imply the oxidation of iron sulfide [13] up to attainment of a sulfur : oxygen ratio of 1 : 1. Therefore, the model structure of oxidized nanoscale mackinawite was obtained by replacing half of the sulfur atoms with oxygen atoms. Calculations in the approximation of density functional theory showed an increase in the band gap by 0.37 eV. This result can explain the appearance of catalytic activity in oxidized nanoscale mackinawite. Based on the simulation, structural models of mackinawite were constructed.

To simulate the structure of catalytically active centers for hydrogen evolution reaction, we constructed three models based on the structure of nanoscale mackinawite, including defects in the substitution of sulfur by oxygen. The first model is the replacement of sulfur atoms with oxygen atoms in the *trans* configuration, the second is replacement in the *cis* configuration, and the third model is replacement in the *cis* configuration, in which hydrogen atoms are located at oxygen atoms. The XANES spectra for the constructed models were calculated. A comparison of the theoretical spectra of crystalline and nanoscale mackinawite is shown in Fig. 2. In the case of nanoscale mackinawite, an increase in the intensity of the main maximum (7122 eV) and a shift of the 7145-eV shoulder toward lower energy values are observed. When considering models with substitutional defects for sulfur atoms by oxygen atoms (Fig. 3), we should note a decrease in the intensity of the main maximum (7122 eV) and its shift by 1.5 eV to high energies, which is consistent with oxidation. The intensity of the maximum at 7145 eV also decreases, which can be explained by a decrease in symmetry. Attention should be paid to the appearance of a pre-edge peak (7117 eV). The spectrum of the structure with a substitutional defect for two sulfur atoms by two oxygen atoms in the *cis* configuration with bonded hydrogen atoms requires special attention. An even greater decrease in the intensity of the main maximum (7124 eV) and the intensity of the pre-edge peak (7114 eV) can be noted.

It should be noted that there are practically no similar studies on the theoretical analysis of XANES spectra at the interface of two-dimensional nanostructured materials. The main advantage of the theoretically

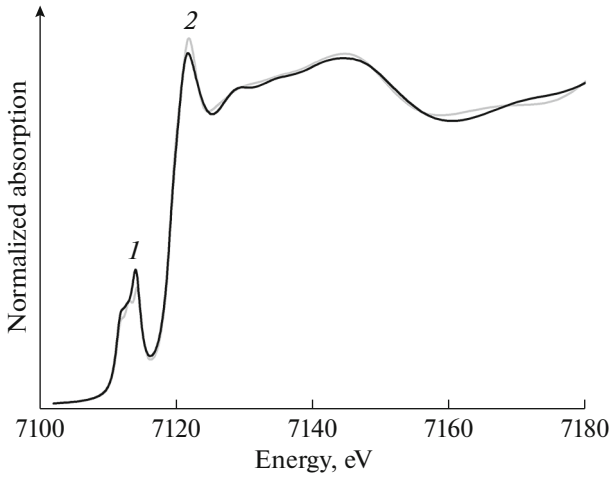

Fig. 2. Theoretical calculation results of the XANES spectrum for (*1*) crystalline and (*2*) nanoscale mackinawite.

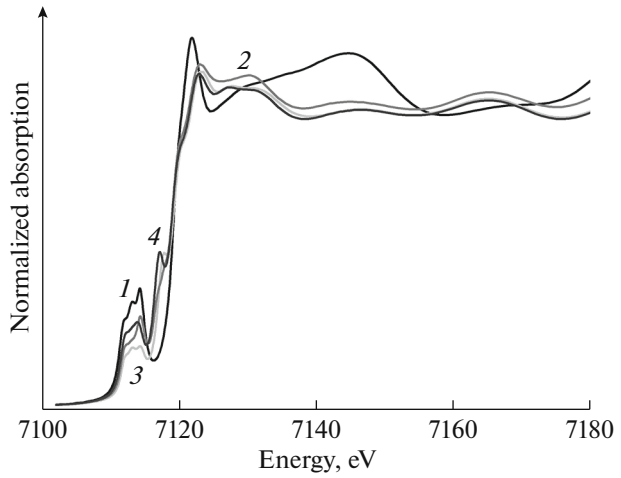

Fig. 3. Theoretical calculation results of the XANES spectrum for (*1*) model structures of nanoscale mackinawite and substitutional defects for two sulfur atoms by oxygen atoms in the (*2*) *trans* and *cis* (*3*) configurations, as well as (*4*) a model that takes into account hydrogen atoms bonded to oxygen atoms in the *cis* configuration.

predicted X-ray absorption spectra XANES is the ability to simulate fundamentally new types of structures that can be realized both statically and in the course of dynamic processes, including in the course of reactions under real technological conditions (in the operando mode). This method allows determination of the parameters of the local atomic structure of materials with a high accuracy when comparing theoretical data with the experiment. This method is the fastest among the analogues available around the world, which allows its application to study the processes of transformation of the local atomic structure of materials in the course of fast processes.

CONCLUSIONS

In this study, we calculated the atomic and electronic structures of iron-sulfide nanosheets, which are new promising two-dimensional nanocatalysts for the hydrogen evolution reaction. The band-gap broadening for the model structure of a mackinawite-based active catalyst compared to nanoscale mackinawite was established as a result of replacement of half of the sulfur atoms with oxygen atoms. The calculated XANES spectra show the sensitivity to changes in the local environment of the iron atom, especially its first coordination sphere. The calculated model structures will allow determination of the features of the local atomic and electronic structure on the mackinawite surface during the hydrogen evolution reaction.

FUNDING

The study was supported by the Russian Foundation for Basic Research, project no. 18-52-53046.

REFERENCES

1. G. R. Walther, E. Post, P. Convey, et al., Nature **416**, 389 (2002). https://doi.org/10.1038/416389a
2. C. Parmesan, Annu. Rev. Ecol., Evol., Systematics **37**, 637 (2006).
3. C. Lesk, P. Rowhani, and N. Ramankutty, Nature **529**, 84 (2016). https://doi.org/10.1038/nature16467
4. D. Kang, T. W. Kim, S. R. Kubota, et al., Chem. Rev. **115**, 12839 (2015). https://doi.org/10.1021/acs.chemrev.5b00498
5. J. H. Huang, Q. C. Shang, Y. Y. Huang, et al., Angew. Chem. **55**, 2137 (2016). https://doi.org/10.1002/anie.201510642
6. D. S. Dhawale, S. Kim, D. H. Park, et al., ChemElectroChem **2**, 497 (2015). https://doi.org/10.1002/celc.201402365
7. R. Miao, B. Dutta, S. Sahoo, et al., J. Am. Chem. Soc. **139**, 13604 (2017). https://doi.org/10.1021/jacs.7b07044
8. M. S. Faber, M. A. Lukowski, Q. Ding, et al., J. Phys. Chem. C **118**, 21347 (2014). https://doi.org/10.1021/jp506288w
9. C. D. Giovanni, A. Reyes-Carmona, A. Coursier, et al., ACS Catal. **6**, 2626 (2016). https://doi.org/10.1021/acscatal.5b02443
10. C. Di Giovanni, W. -A. Wang, S. Nowak, et al., ACS Catal. **4**, 681 (2014). https://doi.org/10.1021/cs4011698
11. Z. Wu, X. Li, W. Liu, et al., ACS Catal, **7**, 4026 (2017). https://doi.org/10.1021/acscatal.7b00466
12. D. Heift, Inorganics **7** (6), 75 (2019). https://doi.org/10.3390/inorganics7060075
13. X. Zou, Y. Wu, Y. Liu, et al., Chem **4**, 1139 (2018). https://doi.org/10.1016/j.chempr.2018.02.023
14. D. Y. Wang, M. Gong, H. L. Chou, et al., J. Am. Chem. Soc. **137**, 1587 (2015). https://doi.org/10.1021/ja511572q
15. A. Martini, S. A. Guda, A. A. Guda, et al., Comput. Phys. Commun. **250**, 107064 (2020). https://doi.org/10.1016/j.cpc.2019.107064
16. M. Franchini, P. H. T. Philipsen, E. van Lenthe, et al., J. Chem. Theory Comput. **10**, 1994 (2014). https://doi.org/10.1021/ct500172n
17. M. Franchini, P. H. T. Philipsen, and L. Visscher, J. Comput. Chem. **34**, 1819 (2013). https://doi.org/10.1002/jcc.23323
18. G. T. Velde and E. J. Baerends, Phys. Rev. B: Condens. Matter Mater. Phys. **44**, 7888 (1991). https://doi.org/10.1103/PhysRevB.44.7888
19. G. Wiesenekker and E. J. Baerends, J. Phys.: Condes. Matter **3**, 6721 (1991). https://doi.org/10.1088/0953-8984/3/35/005
20. G. Wiesenekker, G. Tevelde, and E. J. Baerends, J. Phys. C **21**, 4263 (1988). https://doi.org/10.1088/0022-3719/21/23/012
21. E. S. Kadantsev, R. Klooster, P. L. De Boeij, et al., Mol. Phys. **105**, 2583 (2007). https://doi.org/10.1080/00268970701598063

22. A. D. Becke, Phys. Rev. A: At., Mol., Opt. Phys. **38**, 3098 (1988). https://doi.org/10.1103/PhysRevA.38.3098
23. C. T. Lee, W. T. Yang, and R. G. Parr, Phys. Rev. B: Condens. Matter Mater. Phys. **37**, 785 (1988). https://doi.org/10.1103/PhysRevB.37.785
24. J. M. Tao, J. P. Perdew, V. N. Staroverov, et al., Phys. Rev. Lett. **91**, 4 (2003). https://doi.org/10.1103/PhysRevLett.91.146401
25. M. A. Soldatov, P. V. Medvedev, S. Wei, et al., J. Surf. Invest.: X-Ray, Synchrotron Neutron Tech. **13**, 1028 (2019). https://doi.org/10.1134/s1027451019060193
26. Y. Joly, Phys. Rev. B: Condens. Matter Mater. Phys. **63**, 125120 (2001). https://doi.org/10.1103/PhysRevB.63.125120
27. Y. Joly, J. Synchrotron Radiat. **10**, 58 (2003). https://doi.org/10.1107/s0909049502017211
28. Y. Joly and S. Grenier, in *X-Ray Absorption and X-Ray Emission Spectroscopy: Theory and Applications*, Ed. by J. A. van Bokhoven and C. Lamberti (Wiley, Chichester, 2016), p. 73.
29. S. A. Guda, A. A. Guda, M. A. Soldatov, et al., J. Chem. Theory Comput. **11**, 4512 (2015). https://doi.org/10.1021/acs.jctc.5b00327
30. A. R. Lennie, S. A. T. Redfern, P. F. Schofield, et al., Mineral. Mag. **59** (397), 677 (1995). https://doi.org/10.1180/minmag.1995.059.397.10

Translated by A. Ivanov